Hindawi
Journal of Nanomaterials
Volume 2018, Article ID 6190251, 7 pages
https://doi.org/10.1155/2018/6190251

Research Article

Antimicrobial Nanocomposites Prepared from Montmorillonite/Ag^+/Quaternary Ammonium Nitrate

Lin Zhang,[1,2,3] Jienan Chen,[1,2,3,4] Wenji Yu,[5] Qingfeng Zhao,[1,2,3] and Jin Liu[1,2,3]

[1]*Ministry of Forestry Bioethanol Research Center, Changsha 410004, China*
[2]*Hunan Engineering Research Center for Woody Biomass Conversion, Changsha 410004, China*
[3]*Bioenvironmental Research Institute, Central South University of Forestry and Technology, Changsha 410004, China*
[4]*Transpoints Inc., P.O. Box 141742, Gainesville, FL 32614, USA*
[5]*Research Institute of Wood Industry, Chinese Academy of Forestry, Beijing 100091, China*

Correspondence should be addressed to Jienan Chen; chenjnx@163.com

Received 22 September 2017; Accepted 5 December 2017; Published 1 January 2018

Academic Editor: Leszek A. Dobrzański

Nanocomposites of Ag with organic montmorillonite (Ag-OMMT), Ag with montmorillonite (Ag-MMT), and organic montmorillonite (OMMT) were successfully prepared via a one-step solution-intercalated method. Sodium MMT, silver nitrate, and dimethyl octadecyl hydroxy ethyl ammonium nitrate were used as precursors. X-ray diffraction, Fourier transform infrared spectroscopy, transmission electron microscopy, and energy dispersive spectroscopy analyses confirmed that the MMT layers were intercalated, and Ag^+ was partly reduced to silver nanoparticles with diameters within 10–20 nm in Ag-OMMT. The decomposition temperature of the organic cations in OMMT and Ag-OMMT increased to 220°C, as revealed by differential scanning calorimetry-thermogravimetric analysis. The antimicrobial activity of the nanocomposites was tested by measuring the minimum inhibitory concentration (MIC) and killing rate. The MICs of Ag-OMMT against *Staphylococcus aureus*, *Escherichia coli*, and *Candida albicans* were 0.313, 2.5, and 0.625 mg/mL, respectively. Because of the presence of quaternary ammonium nitrate, Ag-OMMT has a better MIC against Gram-positive bacteria compared to Gram-negative bacteria and fungi. OMMT did not show antimicrobial activity against *Escherichia coli* and *Candida albicans*. In 2 h, 0.0125 mg/mL Ag-OMMT could kill 100% of *S. aureus, E. coli*, and *C. albicans* in solution, and Ag-MMT could kill 99.995% of *S. aureus*, 90.15% of *E. coli*, and 93.68% of *C. albicans*. These antimicrobial functional nanocomposites have the potential for application in the area of surface decoration films.

1. Introduction

Montmorillonite (MMT), an all-purpose clay, is widely used in a range of applications because of its high cation exchange capacity, swelling capacity, high surface areas, and strong adsorption and absorption capacities [1–3]. In recent years, the synthesis and application of MMT-based antibacterial materials have attracted great interest due to global concerns regarding public health. Some researchers have reported modified MMT materials with antibacterial activity. For example, silver, copper, and zinc ions have been immobilized on MMT [4–9], and cetylpyridinium, cetyltrimethylammonium [10–12], tetradecyltrimethylammonium [13], chitosan [14, 15], and chlorhexidine acetate [16] have been intercalated into the MMT layers. In addition, pharmacology studies have revealed that MMT can adsorb to bacteria such as *Escherichia coli (E. coli), Staphylococcus aureus (S. aureus)*, and immobilized cell toxins [17, 18].

Meanwhile, polymers used in several industries such as food processing, biomedical devices, and filtering are required to have antiseptic ability to minimize the transmission of bacterial infections [19]. The dispersibility and compatibility of antimicrobials with polymers is one of the key factors for the preparation of antimicrobial polymers. To improve the compatibility between the antimicrobial and polymer, surface modification of the antimicrobial is required. Furthermore, a lot of researches [20–23] shown that nanoparticles, such as clay and graphene nanoplatelets which was incorporated in antimicrobial polymer nanocomposites, allowed for the tuning of the release of antimicrobial agents,

Table 1: d_{001} of MMT modified with different organic cations.

Sample	MMT	Ag-MMT	OMMT	2.25 mmol Ag-OMMT	4.5 mmol Ag-OMMT	6.75 mmol Ag-OMMT	9.0 mmol Ag-OMMT	11.25 mmol Ag-OMMT
$2\theta_{001}/^{\circ}$	7.019	6.396	4.460	4.498	4.480	4.360	4.419	4.418
d_{001}/nm	1.258	1.381	1.980	1.963	1.971	2.025	1.998	1.998

especially reducing the burst release effect, without hindering the antimicrobial activity of the obtained materials.

The aim of this work was to prepare organic antiseptic MMT with good compatibility and dispersibility for use as a nanoadditive in polymers. For this purpose, MMT was modified with Ag^+ and quaternary ammonium nitrate via a one-step solution-intercalation technique. The structures of different antimicrobial organic MMTs were characterized by X-ray diffraction (XRD), Fourier transform infrared spectroscopy (FTIR), scanning electron microscopy (SEM), transmission electron microscopy (TEM), and energy dispersive spectroscopy (EDS) techniques, and the thermal stability was confirmed by differential scanning calorimetry-thermogravimetric (DSC-TG) analysis. The antimicrobial activity of the nanocomposites was evaluated by examining the minimum inhibitory concentration (MIC) and killing rate.

2. Experimental

2.1. Materials. Sodium MMT used in this study was supplied by Zhejiang Fenghong Clay Chemicals Co., Ltd (China). The cation exchange capacity (CEC) of MMT was 90 meq $(100\,g)^{-1}$. Silver nitrate ($AgNO_3$) with a purity of 99.8% was provided by Hunan Hipure Chemical Reagent Factory (China). Dimethyl octadecyl hydroxy ethyl ammonium nitrate (DOHEAN) at 50% (w/w) in butanol was provided by Jiangsu Hai'an Petrochemical Plant (China). Other reagents used in this study were of analytical grade.

2.2. Synthesis of Antimicrobial Organoclays. 10 g sodium MMT was dispersed in 200 mL deionized water and stirred at 80°C. $AgNO_3$ (equimolar with the CEC) was dissolved in deionized water and then slowly dropped into the MMT sol, which was then kept at 80°C for 1 h with stirring. An equimolar quantity of DOHEAN was added to the Ag^+ and MMT sol and kept at 80°C for 2 h with stirring. The intercalated montmorillonite (Ag-OMMT) was repeatedly washed with deionized water to remove residual $AgNO_3$ and DOHEAN. This composite was then dried at 100°C for 24 h and then ground to a size less than 300 mesh.

The preparation of Ag-MMT and OMMT were consistent with the above methods but absented the process of addition $AgNO_3$ and DOHEAN, respectively.

2.3. Measurements. XRD measurements were performed using a D/Max 2550 diffractometer (Rigaku Electrical Co., Ltd.) with a Cu target and K_α radiation (λ = 0.154 nm). TG and DSC curves were recorded at 20–800°C with a heating rate of 10°C/min under N_2 (Netzsch STA 449 C). FTIR spectra were collected from KBr pressed disks on a Nicolet 380 spectrophotometer. SEM images were recorded with a JEOL JSM-6380LV microscope, and TEM and EDS characterizations were performed on a Tecnai G2 20 FEI AEM.

2.4. Evaluation of Antimicrobial Activity. Gram-positive bacteria *Staphylococcus aureus*, Gram-negative bacteria *Escherichia coli*, and fungi *Candida albicans* were provided by the China Center of Industrial Culture Collection (CICC at Beijing).

2.4.1. Minimum Inhibitory Concentration [24]. MIC tests were performed in MHA for the bacteria and fungi. A serial twofold dilution of Ag-OMMT was added to an equal volume of medium to obtain a concentration of 5000 μg/mL, which was serially diluted by double technique to achieve solutions of 2500–9.77 μg/mL. Control dishes containing equal volumes of distilled water were also prepared. After cooling and drying, the plates were inoculated with 2 μL of 10^7 CFU/mL strain solutions and incubated aerobically at 27°C for 16–20 h for bacteria or 72–96 h for fungi. Growth control samples of each tested strain were also included. The MIC was defined as the lowest concentration required to inhibit bacterial growth, that is, the concentration at which <5 microorganism colonies were visible.

2.4.2. Antimicrobial Killing Rate [24]. The microorganism suspension was diluted using 0.9% (w/v) sterile saline water to 10^4 CFU/mL. 1 mL of cell suspension was added to 95 mL of 0.05, 0.025, and 0.0125 mg/mL nanocomposite (Ag-MMT and Ag-OMMT) solutions that had been autoclaved at 121°C for 20 min. Nanoscale SiO_2 was used as a control. The samples were removed after 2 h shake cultivation. 50 μL aliquots were spread on nutrient agar plates, which were incubated at 37°C for 24 h, and the numbers of colonies were counted for each solution. The percent reductions in plate colony counts were calculated by comparing the experiment plates to the control. All presented data were averaged from at least 3 parallel experiments, where the discrepancies among them were <5%.

3. Results and Discussion

3.1. Structure and Morphology. The XRD patterns of unmodified MMT, Ag-MMT, OMMT, and Ag-OMMTs (modified with different amounts of Ag^+) are presented in Figure 1. Table 1 shows the d-spacing of 001 (d_{001}) for MMT as calculated by Bragg's equation [25]. Ag-MMT features a larger basal spacing (1.381 nm) than MMT (1.258 nm), indicating that Ag^+ was exchanged in the silicate layers. Both OMMT and Ag-OMMT feature wide basal spacings with

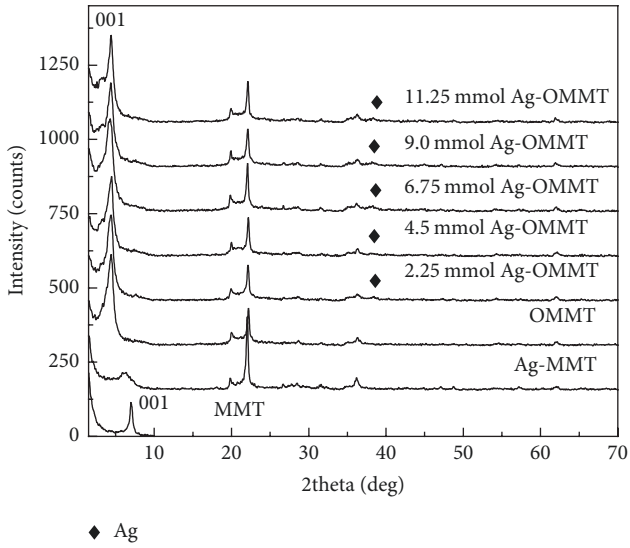

Figure 1: XRD patterns of MMT, Ag-MMT, OMMT, and Ag-OMMTs with different amounts of Ag^+. MMT: unmodified MMT; Ag-MMT: MMT modified with Ag; OMMT: MMT modified with DOHEAN; Ag-OMMT: MMT modified with Ag and DOHEAN.

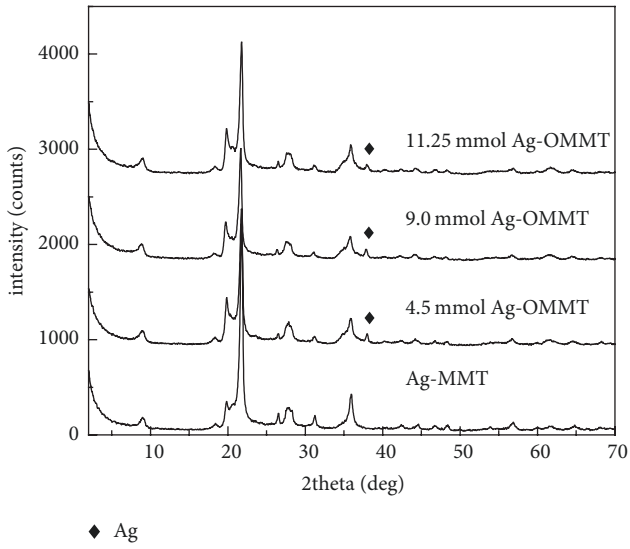

Figure 2: XRD patterns of Ag-MMT and Ag-OMMTs (different amounts of Ag^+) after calcination at 750°C for 2 h. MMT: unmodified MMT; Ag-MMT: MMT modified with Ag; OMMT: MMT modified with DOHEAN; Ag-OMMT: MMT modified with Ag and DOHEAN.

high d_{001} values between 1.96 nm and 2.03 nm, indicating that DOHEAN has been intercalated into the MMT layers.

As shown in Figure 1, minimal metallic silver is present in all the Ag-OMMTs (at $2\theta = 38^\circ$) but is absent in Ag-MMT. This is also noted in Figure 2, which shows the XRD patterns of Ag-MMT and Ag-OMMTs having different amounts of Ag^+ after calcination at 750°C for 2 h. In the presence of easily oxidizable organic cations, Ag^+ as an oxidant was partly reduced to metallic silver during the preparation process; after high temperature calcination, the reaction of Ag^+ and DOHEAN was complete. However, in the absence of organic cation, Ag^+ could not easily be deoxidized, even after calcination at 750°C. This has also been demonstrated by EDS (Figure 3).

Figure 3 shows the EDS pattern of Ag-OMMT and the morphologies of Ag-MMT and Ag-OMMT. The modified MMTs appear as sandwich-like crystals in the TEM images. Numerous black spots are homogeneously dispersed in the MMT crystals, as shown in Figure 3(b), which are metallic silver nanoparticles as demonstrated by EDS and XRD analyses. These silver nanoparticles are smaller in Ag-MMT (particle diameter within 2–5 nm, Figure 3(a)) than in Ag-OMMT (particle diameter within 10–20 nm, Figure 3(a)) because Ag^+ is more easily deoxidized in the presence of organic cations; this is in agreement with the XRD results (Figures 1 and 2). Figure 4 presents SEM micrographs showing the morphology change of MMT before and after modification. Unmodified MMT (Figure 4(a)) has a compact and flat surface, while, after modification, the MMT surface becomes crinkled and rough with wide interspacing (Figure 4(b)), which is desirable for use as a nanoadditive.

3.2. DSC-TG. DSC-TG curves of DOHEAN, MMT, Ag-MMT, OMMT, and Ag-OMMT are shown in Figure 5. The TG curve of each sample shows an endothermal peak below 100°C with a corresponding weight-loss due to the removal of water. The DSC curves of MMT and Ag-MMT both feature a second endothermal peak at 679.2°C and 674°C, respectively, corresponding to the loss of hydrated water of the interlayer cations and the structural hydroxyls [26].

The sharp exothermal peak on the DSC curve of DOHEAN represents the evaporation or decomposition of DOHEAN. However, there are two exothermal peaks on the DSC curves of OMMT and Ag-OMMT. The low-temperature exothermal peak corresponds to the evaporation or decomposition of DOHEAN on the silicate plate surfaces, and the other peak represents the evaporation or decomposition of DOHEAN between the silicate plates. The TG curves of OMMT and Ag-OMMT reveal that the evaporation or decomposition of DOHEAN occurs at approximately 220°C, which is higher than that of pure DOHEAN (160°C). This indicates that the organic cation has intercalated into the MMT layers, similar to the initial state, and that the silicate platelets have the ability to protect organic molecules from decomposition. [27]. A similar behavior was reported by Scaffaro et al. [28] during the preparation of poly(ethylene-co-vinyl acetate) films with two commercial formulations of nisin.

3.3. FTIR. Figure 6 shows the FTIR spectra of MMT, DOHEAN, Ag-MMT, OMMT, and Ag-OMMT. Compared to MMT, OMMT has additional absorption peaks appearing at 2921, 2850, and 1384 cm^{-1}. The peaks at 2921 and 2850 cm^{-1} arise from $-CH_2-$ and $-CH_3$ stretching vibrations, while the one at 1384 cm^{-1} belongs to C–H symmetric deformation vibrations [29]. This further reveals that DOHEAN has intercalated into the MMT layers. The peak at 3100–3700 cm^{-1} represents O–H stretching vibrations [30] and the peak at 1638 cm^{-1} belongs to H–O–H bending vibrations [31]. This

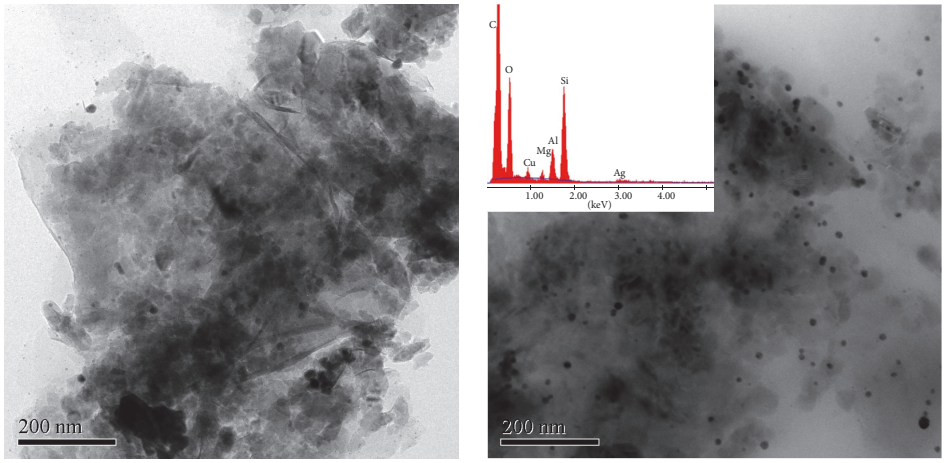

(a) TEM of Ag-MMT (b) TEM and EDS of Ag-OMMT

Figure 3: EDS pattern of Ag-OMMT and TEM micrographs of Ag-MMT and Ag-OMMT.

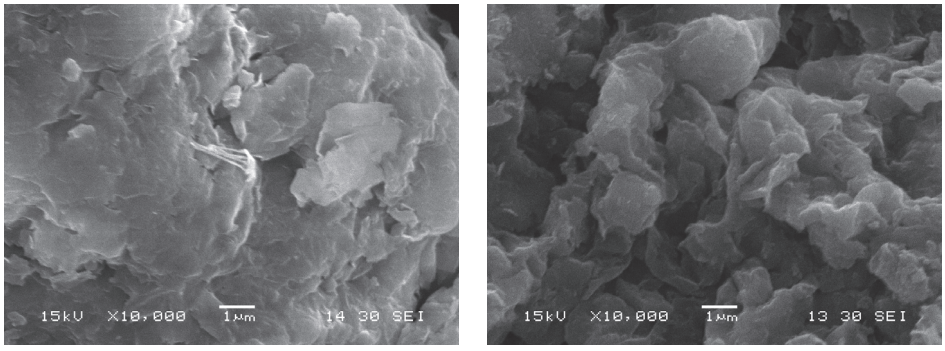

(a) MMT (b) Ag-OMMT

Figure 4: SEM micrographs of MMT and Ag-OMMT.

Table 2: MIC of the samples.

Samples	MIC (mg/mL)		
	S. aureus	*E. coli*	*C. albicans*
Ag-MMT	1.25	2.5	0.625
OMMT	2.5	>40	>40
Ag-OMMT	0.313	2.5	0.625

band, which is related to the ν_2(H–O–H) bending vibration of water adsorbed on MMT, shifted from 1631 cm^{-1} in MMT to 1638 cm^{-1} for Ag-OMMT. Meanwhile, the intensity of this band decreased, reflecting that the amount of water adsorbed on MMT decreased after modification of the MMT with organic cations.

3.4. Antimicrobial Activity Assay. As shown in Table 2, Ag-MMT and Ag-OMMT have obvious antimicrobial activity against a wide variety of microorganisms, including Gram-positive bacteria, Gram-negative bacteria, and fungi. They have the same MIC for *E. coli* and *C. albicans*, which are 2.5 and 0.625 mg/mL, respectively. In addition, Ag-OMMT has a higher MIC (0.313 mg/mL) for *S. aureus* than Ag-MMT (1.25 mg/mL). Strong antimicrobial activity was also observed, as outlined in Table 3. At a concentration of 0.0125 mg/mL, Ag-OMMT can kill 100% of the *S. aureus, E. coli*, and *C. albicans* population in 2 h, and Ag-MMT can kill 99.995% of the *S. aureus*, 90.15% of *E. coli*, and 93.68% of *C. albicans* in 2 h.

OMMT can inhibit the growth of *S. aureus*; however, its ability to inhibit the growth of *E. coli* and *C. albicans* is less pronounced. This phenomenon is due to the different cell structures of these microbes. *S. aureus*, a Gram-positive bacterium, consists of a thick peptidoglycan layer and a cytoplasmic membrane. Its peptidoglycan layer is extensively crosslinked in three dimensions to form a solid mesh. Despite its thickness, the peptidoglycan layer of Gram-positive bacteria is not a barrier to the diffusion of foreign molecules. Gram-negative bacteria, however, have a small layer of peptidoglycan and an outer membrane made of a toxic liposaccharide layer. Because of this structure, Gram-negative bacteria are unusually permeable to foreign molecules. Therefore, Gram-negative bacteria are generally less susceptible to antibiotics and antibacterial agents than Gram-positive bacteria [32].

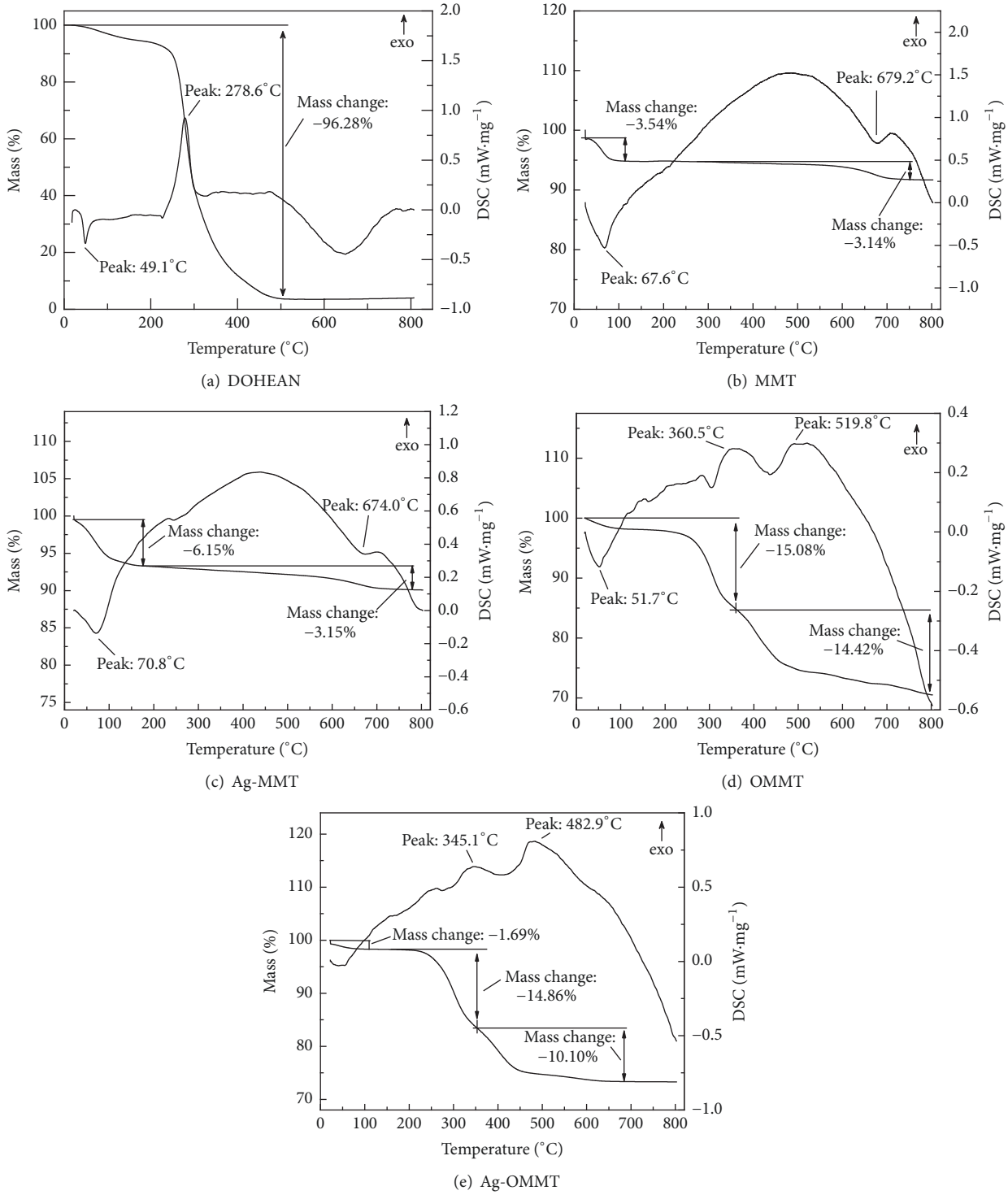

Figure 5: DSC-TG profiles of DOHEAN, MMT, Ag-MMT, OMMT, and Ag-OMMT.

Table 3: Killing rate of the samples.

C_{sample}/(mg·Ml^{-1})	Killing rate/%					
	S. aureus		*E. coli*		*C. albicans*	
	Ag-MMT	Ag-OMMT	Ag-MMT	Ag-OMMT	Ag-MMT	Ag-OMMT
0.05	100	100	100	100	100	100
0.025	100	99.996	100	99.99	100	99.996
0.0125	100	99.995	100	90.15	100	93.68

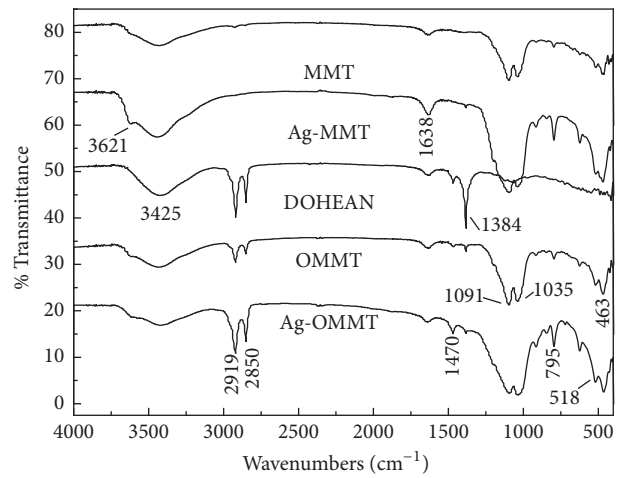

Figure 6: FTIR spectra of MMT, DOHEAN, Ag-MMT, OMMT, and Ag-OMMT.

4. Conclusions

Novel antimicrobial nanocomposites featuring sodium MMT, Ag^+, and dimethyl octadecyl hydroxy ethyl ammonium nitrate were synthesized via a one-step solution-intercalated method. XRD, DSC-TG, FTIR, SEM, TEM, and EDS characterization indicated that Ag^+ and DOHEAN were intercalated into the MMT layers. Ag formed both metallic species and Ag^+ in the clay layer, while DOHEAN was chemically bonded with the MMT layers. The thermal stability of DOHEAN was improved by the protection from the MMT layers. The nanocomposite surface became crinkled and rough after modification, making it suitable for combining with polymers. Further, the nanocomposites showed a wide range of highly efficient antimicrobial activity. The results of this study may be used as a foundation for the future development of new types of nanocomposites of antimicrobial polymers in many industries, such as in wood adhesives, plastics, paints, and rubbers.

Conflicts of Interest

The authors declare that they have no conflicts of interest.

Acknowledgments

This work was supported by the National Special Program for International Science and Technology Cooperation (no. 2015DFA01120), the Hunan Province Major Program of Science and Technology (2017NK1010), the Key Projects in the National Science & Technology Pillar Program during the Eleventh Five-year Plan Period of China (2006BAD07A07-08), and the Hunan Province Natural Science Foundation (2015JJ5007).

References

[1] R. K. Gogoi and K. Raidongia, "Strategic shuffling of clay layers to imbue them with responsiveness," *Advanced Materials*, vol. 29, no. 24, Article ID 1701164, 2017.

[2] J. L. Suter, D. Groen, and P. V. Coveney, "Chemically specifi C multiscale modeling of clay-polymer nanocomposites reveals intercalation dynamics, tactoid self-assembly and emergent materials properties," *Advanced Materials*, vol. 27, no. 6, pp. 966–984, 2015.

[3] X. Wang, B. Liu, and P. Yu, "Research on the Preparation and Mechanism of the Organic Montmorillonite and Its Application in Drilling Fluid," *Journal of Nanomaterials*, vol. 2015, Article ID 514604, 10 pages, 2015.

[4] S. Sh, M. Rassa, and D. E. Mohammadi, "Spectroscopic study of silver halides in montmorillonite and their antibacterial activity," *Journal of Photochemistry and Photobiology B: Biology*, vol. 163, pp. 150–155, 2016.

[5] C. Perrine, G. Fabrice, and E. Eliane, "Preparation, characterization and barrier properties of silver/montmorillonite/starch nanocomposite films," *Journal of Membrane Science*, vol. 497, pp. 162–171, 2016.

[6] J. F. Martucci and R. A. Ruseckaite, "Antibacterial activity of gelatin/copper (II)-exchanged montmorillonite films," *Food Hydrocolloids*, vol. 64, pp. 70–77, 2017.

[7] L. F. Jiao, Y. L. Ke, K. Xiao, Z. H. Song, J. J. Lu, and C. H. Hu, "Effects of zinc-exchanged montmorillonite with different zinc loading capacities on growth performance, intestinal microbiota, morphology and permeability in weaned piglets," *Applied Clay Science*, vol. 112-113, pp. 40–43, 2015.

[8] T. Li, O. Lin, Z. Lu, L. He, and X. Wang, "Preparation and characterization of silver loaded montmorillonite modified with sulfur amino acid," *Applied Surface Science*, vol. 305, pp. 386–395, 2014.

[9] S. Sohrabnezhad, M. Rassa, and A. Seifi, "Green synthesis of Ag nanoparticles in montmorillonite," *Materials Letters*, vol. 168, pp. 28–30, 2016.

[10] G. Özdemir, S. Yapar, and M. H. Limoncu, "Preparation of cetylpyridinium montmorillonite for antibacterial applications," *Applied Clay Science*, vol. 72, pp. 201–205, 2013.

[11] Y. L. Ke, L. F. Jiao, Z. H. Song et al., "Effects of cetylpyridinium-montmorillonite, as alternative to antibiotic, on the growth performance, intestinal microflora and mucosal architecture of weaned pigs," *Animal Feed Science and Technology*, vol. 198, pp. 257–262, 2014.

[12] P. Herrera, R. Burghardt, H. J. Huebner, and T. D. Phillips, "The efficacy of sand-immobilized organoclays as filtration bed materials for bacteria," *Food Microbiology*, vol. 21, no. 1, pp. 1–10, 2004.

[13] B. K. G. Theng, J. Aislabie, and R. Fraser, "Bioavailability of phenanthrene intercalated into an alkylammonium-montmorillonite clay," *Soil Biology & Biochemistry*, vol. 33, no. 6, pp. 845–848, 2001.

[14] S. Bensalem, B. Hamdi, S. Del Confetto et al., "Characterization of chitosan/montmorillonite bionanocomposites by inverse gas chromatography," *Colloids and Surfaces A: Physicochemical and Engineering Aspects*, vol. 516, pp. 336–344, 2017.

[15] V. Ambrogi, D. Pietrella, M. Nocchetti et al., "Montmorillonite–chitosan–chlorhexidine composite films with antibiofilm activity and improved cytotoxicity for wound dressing," *Journal of Colloid and Interface Science*, vol. 491, pp. 265–272, 2017.

[16] K. Saha, B. S. Butola, and M. Joshi, "Synthesis and characterization of chlorhexidine acetate drug-montmorillonite intercalates for antibacterial applications," *Applied Clay Science*, vol. 101, pp. 477–483, 2014.

[17] P. Herrera, R. C. Burghardt, and T. D. Phillips, "Adsorption of *Salmonella enteritidis* by cetylpyridinium-exchanged montmorillonite clays," *Veterinary Microbiology*, vol. 74, no. 3, pp. 259–272, 2000.

[18] Y. Zhou, M. Xia, Y. Ye, and C. Hu, "Antimicrobial ability of Cu^{2+}-montmorillonite," *Applied Clay Science*, vol. 27, no. 3-4, pp. 215–218, 2004.

[19] H. Weickmann, J. C. Tiller, R. Thomann, and R. Mülhaupt, "Metallized organoclays as new intermediates for aqueous nanohybrid dispersions, nanohybrid catalysts and antimicrobial polymer hybrid nanocomposites," *Macromolecular Materials and Engineering*, vol. 290, no. 9, pp. 875–883, 2005.

[20] R. Scaffaro, L. Botta, A. Maio, and G. Gallo, "PLA graphene nanoplatelets nanocomposites: Physical properties and release kinetics of an antimicrobial agent," *Composites Part B: Engineering*, vol. 109, pp. 138–146, 2017.

[21] R. Scaffaro, L. Botta, A. Maio, M. C. Mistretta, and F. P. La Mantia, "Effect of graphene nanoplatelets on the physical and antimicrobial properties of biopolymer-based nanocomposites," *Materials*, vol. 9, no. 5, article 351, 2016.

[22] V. H. Campos-Requena, B. L. Rivas, M. A. Pérez, K. A. Garrido-Miranda, and E. D. Pereira, "Polymer/clay nanocomposite films as active packaging material: modeling of antimicrobial release," *European Polymer Journal*, vol. 71, pp. 461–475, 2015.

[23] C. Viseras, C. Aguzzi, P. Cerezo, and M. C. Bedmar, "Biopolymer-clay nanocomposites for controlled drug delivery," *Materials Science and Technology*, vol. 24, no. 9, pp. 1020–1026, 2013.

[24] GB/T21510-2008, Antimicrobial property detection method for nano-inorgnic materials.

[25] S. M. M. Meira, G. Zehetmeyer, A. I. Jardim, J. M. Scheibel, R. V. B. de Oliveira, and A. Brandelli, "Polypropylene/montmorillonite nanocomposites containing nisin as antimicrobial food packaging," *Food and Bioprocess Technology*, vol. 7, no. 11, pp. 3349–3357, 2014.

[26] H. He, Z. Ding, J. Zhu et al., "Thermal characterization of surfactant-modified montmorillonites," *Clays and Clay Minerals*, vol. 53, no. 3, pp. 287–293, 2005.

[27] R. Scaffaro, L. Botta, A. Frache, and F. Bellucci, "Thermo-oxidative ageing of an organo-modified clay and effects on the properties of PA6 based nanocomposites," *Thermochimica Acta*, vol. 552, pp. 37–45, 2013.

[28] R. Scaffaro, L. Botta, S. Marineo, and A. M. Puglia, "Incorporation of nisin in poly (ethylene-co-vinyl acetate) films by melt processing: a study on the antimicrobial properties," *Journal of Food Protection*, vol. 74, no. 7, pp. 1137–1143, 2011.

[29] A. Moslemizadeh, S. Khezerloo-ye Aghdam, K. Shahbazi, H. Khezerloo-ye Aghdam, and F. Alboghobeish, "Assessment of swelling inhibitive effect of CTAB adsorption on montmorillonite in aqueous phase," *Applied Clay Science*, vol. 127-128, pp. 111–122, 2016.

[30] H. Slosiariková, J. Bujdák, and V. Hlavatý, "IR Spectra of octadecylammonium-montmorillonite in the range of the Si-O Vibrations," *Journal of Inclusion Phenomena and Molecular Recognition in Chemistry*, vol. 13, no. 3, pp. 267–272, 1992.

[31] L. Jiao, F. Lin, S. Cao, C. Wang, H. Wu, and M. Shu, "Preparation, characterization, antimicrobial and cytotoxicity studies of copper/zinc- loaded montmorillonite," *Journal of Animal Science Biotechnology*, vol. 8, no. 1, p. 27, 2017.

[32] H. Liu, Y. Du, J. Yang, and H. Zhu, "Structural characterization and antimicrobial activity of chitosan/betaine derivative complex," *Carbohydrate Polymers*, vol. 55, no. 3, pp. 291–297, 2004.